Surface Modification of Space Materials Induced by Low Energetic Particle Irradiation

Denise Beisecker[1]
[1]*German Aerospace Center DLR, Institute of Technical Physics, Stuttgart, Germany*
Frederic Seiz[1], **Nils Bartels**[1], **Wolfgang Riede**[1], **Maciej Sznajder**[2], **Thomas Renger**[2], **Tom Spröwitz**[2]
[1]*German Aerospace Center DLR, Institute of Technical Physics, Stuttgart, Germany*
[2]*German Aerospace Center DLR, Institute of Space Systems, Bremen, Germany*

ABSTRACT

A set of six different materials frequently used in spacecraft engineering was irradiated with low energy (100 keV) proton irradiation to simulate the aging of their surfaces due to space radiation in Low Earth Orbit. A microscopic and spectroscopic analysis of the irradiated samples reveals that the tested materials containing organic polymers Polytetrafluoroethylene (PTFE) and carbon fiber reinforced plastic (CFRP) show significant changes in surface morphology. As opposed to this, samples with a metallic surface such as aluminum, titanium or multi-layer insulation (MLI) remain rather unaffected. This knowledge is highly relevant for the interpretation of optical data related to the observation of space debris (so-called “light curves”) as well as to studies about laser matter interaction for laser-based debris removal.

1. INTRODUCTION

Although most of the satellite missions since 2007 follow the agreement of deorbiting satellites at their end of life [1], satellite operators have to deal with a high amount of space debris [2]. In cases of potential collisions, satellite operators can react by initiating collision avoidance maneuvers. Between the years 2005 to 2014, the number of collision avoidance maneuvers has increased by a factor of eight [3]. Unfortunately, collision avoidance maneuvers are quite costly and most debris fragments smaller than 10 cm are not detected and catalogued and thus cannot be avoided [4]. To improve this situation, space organizations like NASA, ESA and JAXA are working on data bases of space debris, trying to gather as much information as possible [5]. Even for a scenario in which 90% of all space missions follow the mitigation standards, collisions of space debris are expected to lead to an increase in the space debris population in Low Earth Orbit (LEO) by 30% over the next 200 years. [6] This suggests that active strategies for debris removal might become necessary to preserve the near Earth environment for future space missions.

An approach, for gathering additional information about the space debris environment in the Low Earth Orbit is extracting data from debris-reflected sunlight with telescopes, so called light curves [7]. These light-curves are often measured with spectral or polarization sensitive detectors [8]. Results are then compared to computer simulations to extract more details of space objects, such as their rotational period, their shape or their surface materials [9]. As a prerequisite for these simulations, it is necessary to provide the computer models with parameters for the reflectivity of different space materials, often resolved with respect to the incidence and scattered angle (so-called bidirectional reflectance distribution function, BRDF) and as a function of polarization and wavelength [10]. While this is already a difficult task in itself, a major additional challenge is that it can be insufficient to measure the reflectivity of space materials on Earth, since material properties might change during the exposure to the space environment [11].
Various studies have been performed investigating surface degradation due to UV light [12], atomic oxygen [13] and particle irradiation [14], [15]. The results of these studies consistently show that the space environment can induce significant changes to optical and mechanical parameters. During the mission MISSE [13], a set of a 168 materials was exposed for 18 months on the exterior of the International space station (ISS). It should, however, be noted that the space radiation at the ISS (~400 km orbital height) is dominated by atomic oxygen and UV solar radiation.

Rarely investigated are the changes of material properties due to low energetic proton and electron irradiation as encountered in the Inner Van-Allen-Belt, which reaches from 1.3 to 1.8 Earth radii. This radiation belt is dominated by positively charged particles (protons) originating from the sun with a kinetic energy in the range of several keV up to 400 MeV [16]. The peak in space traffic appears at 800 km height, which directly intersects with the Inner Van-Allen-Belt [17].

In this work we study the degradation of several materials due to energetic protons as encountered in the inner van-Allen belt. A focus is on low energetic particles (~100 keV) since these particles are known to cause most severe surface modifications as they are stopped near the surface of the spacecraft material. [18] The goal of this work is to conclude how and for which materials properties such as the surface morphology and reflectivity are affected by the proton irradiation.

2. METHODS

To investigate the effects of low energetic particle irradiation on material surfaces, we performed space aging experiments at the Complex Irradiation Facility (CIF) at the German Aerospace Center (DLR) in Bremen. Here, the main focus was on proton irradiation. The samples were investigated before and after radiation with an incident light- and a scanning electron microscopy, in order to detect possible changes to the surface morphology. We also performed an in-situ measurement of the reflectivity at 632 nm using a measurement system, which we called LAMBDA.
In the following, we briefly introduce the applied systems.

2.1. Complex Irradiation Facility

The CIF is an experimental set-up designed to simulate low energetic space radiation and its impact on spacecraft material surfaces. As radiation sources it uses a sun simulator consisting of Xenon, Deuterium and Argon light sources as well as particle accelerators providing protons and electrons, which are linked to an ultra-high vacuum sample chamber, see Fig. 1. The sample chamber is equipped with a temperature-controlled sample holder system. The facility can either provide any radiation component separately or combined. CIF can simulate a solar flux op to several solar constants and accelerated charged particles (protons and electrons) to a maximum kinetic energy of 100 keV [19]. The facility is intentionally designed for the investigation of radiation effects on surface materials [20]. It has proven its value already in other research projects, mainly concerning deorbit sails and solar sailing [21].

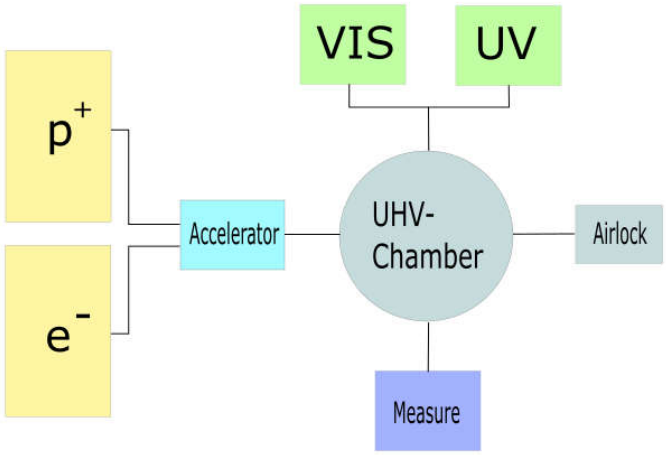

Fig. 1: Schematic of the Complex Irradiation Facility

2.2. LAMBDA – Laser cAMera alBeDo Analyzer

LAMBDA is a device we specifically designed for this work. It allows for an in-situ measurement of the relative reflectivity change at 632 nm under a given angle of material surfaces during the irradiation in the CIF. The system consists of a HeNe-Laser, a Canon EOS 5D Mark IV camera and a beam expanding lens system, which is arranged as depicted in Fig. 2. Due to the geometry of the sample chamber, the laser beam, the camera axis and the proton beam are arranged under 30° to each other.
The measurement principle works as follows: Red laser light is emitted by a low power HeNe laser. The expanded beam spot illuminates the samples inside the UHV-chamber while they are under charged particle irradiation. Since the reflection is depending on the condition of a surface the reflectivity per spatial angle is changing. This change is detected by the camera. Calculating the average relative luminescence of the pixels gives information about the reflected light which is directed towards the camera. The charged particle irradiation time can be related to an orbit equivalent time. This leads to the conclusion how much a surface decays depending on orbit and time.

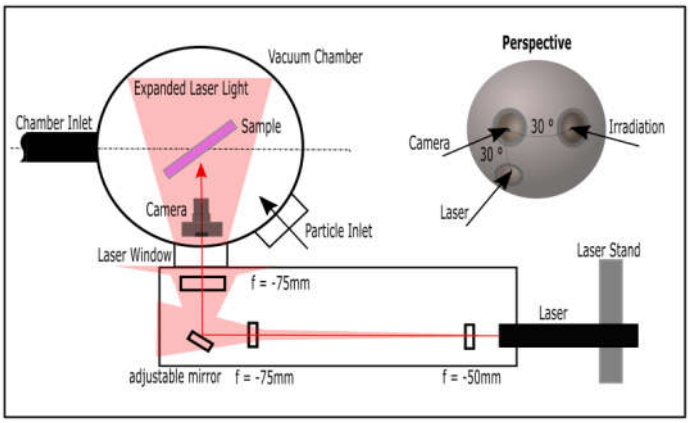

Fig. 2: Schematic Principle of LAMBDA

2.3. Microscopes

The microscopic inspection of the optical surfaces before and after irradiation in the CIF was performed with an incident light microscope, which is a Keyence Digital Microscope Type VHX-7000 Series.
Furthermore, we use a scanning electron microscope (SEM, Zeiss type EVO MA 10) to detect surface modifications at high magnification.

2.4. Spectral Analysis

A Fourier-Transform Infrared Spectrometer (FTIR) Bruker Vertex70v has been used to analyze the normal reflectance spectra of the reference sample and the irradiated sample in the wavelength range from 0.4 µm to 10 µm. The visible range between 0.4 µm and 1.0 µm was measured using a tungsten light source combined with a silicon diode and the range 1.2 µm to 10 µm with the internal Globar light source and a room temperature DTGS diode.

3. Experiment

3.1. Samples

Fig. 3 shows the sample holder used for the irradiation in the CIF. It carries 6 samples with the size of 21x21 mm² each. The samples, which are CFRP, Aluminum, ITO coated MLI, AcktarBlack coated aluminum foil, Titanium and PTFE, are listed in Table 1. These materials are frequently used in spacecraft engineering and represent different material groups.

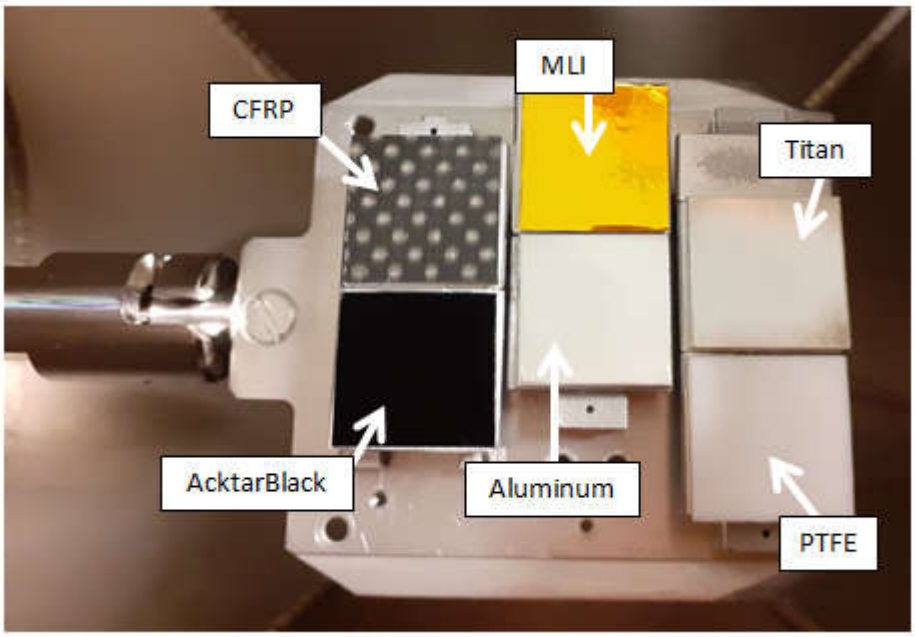

Fig. 3: Sample Set

Table 1: Properties of Material Choice

Material	Description	Category
Carbon Fiber Reinforced Plastic (CFRP)	Fiber Fabric (canvas) with Epoxy resin 1mm thickness	Polymer, black
AcktarBlack	Type: Spectral Black™ Layer thickness: 3 – 7µm on 125µm Aluminum foil 99.5 – 99.7% absorbtivity for wavelength range 0.3 – 14µm	Metal, black
Multilayer Insulation with indium tin oxide	Stack: ITO – Kapton – Aluminum Type: Sheldahl No 1473623	Polymer, polished metal surface (golden)
Aluminum 6082	2mm thick material with polished surface	Metal, polished metals surface
Titan	0.8mm thick material with polished surface	Metal, polished metals surface
Polytetrafluorethylene (PTFE, Teflon)	Commercially available material with 1mm thickness	Polymer, white

3.2. Irradiation parameters

We decided to perform our irradiation tests using an irradiation dose representative for an orbital height of 800 km, as this is where a majority of objects in Low Earth Orbit are resident [17]. The most populated inclination at this orbital height is the sun synchronous orbit. In this orbit, the amount of atomic oxygen is almost zero, whereas the density of charged particles (protons and electrons) is rather high. This density of protons (p^+) and electrons (e^-) was estimated using SPENVIS (SPace ENVironment Information System), where AE8 and AP8 models have been used to calculate the electron and proton fluxes, respectively [22].

In Fig. 4 we display the integrated fluence (y-axis) over the particle energy (x-axis). The fluence sums up all particles per centimeter square, which are on a chosen level and above. We calculated both extreme cases during the sun cycle, which is the solar maximum (solid lines), where the peaks in giant particle and mass eruptions, and the solar minimum (dotted lines), where the sun activity is low and calm. We found that the fluencies of electrons (blue lines) and protons (black lines) are on a comparable level during the sun cycle. The largest proton fluence equals to 2.2×10^{13} p^+ cm^{-2} and corresponds to proton energy of 100 keV. TheCIF has ability to produce protons with maximum kinetic energy of 100 keV. Its maximum effective exposure area is 6.2 x7.3 cm^2. If one takes a current of 0.1 µA (6.24×10^{11} p^+ s^{-1}) then the flux over the area is 1.37×10^{11} p^+ cm^{-2} s^{-1}. Under these conditions, 100 years in LEO's 800 km SSO orbit are simulated in 26.6 minutes.

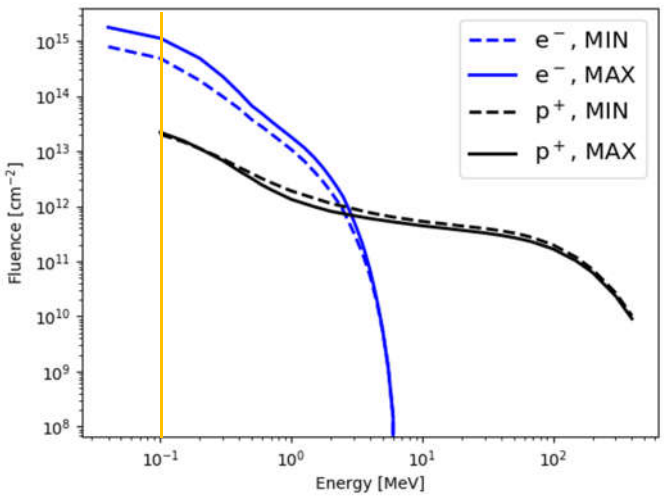

Fig. 4: Electron and proton fluence of equivalent of 100 years in the 800 km LEO orbit

In orbit, any material will encounter a continuous spectrum of particles with different kinetic energy over a period of several years. As opposed to this, the CIF will generate mono-energetic particle radiation and the dose will have to be applied over short time. As we are interested in changes to the optical surface, we decided- in an initial step - to irradiate samples with protons of a kinetic energy of 100 keV, since there are reliable models to estimate the irradiation dose and since the penetration depth lies between 0.6 and 1.1 µm in the investigated materials, depending on the material properties, it is likely to induce surface modifications. The irradiation dose was chosen to 100 keV at 100 nA for 26.6 min, which represents an in-orbit duration of 100 years at 800 km SSO. The expectable errors are listed in Table 2 below.

Table 2: Measurement Errors during the irradiation procedure

Error Source	Nominal Value	Error Range
Sample Size	6.4 x 7.4 cm	± 2 mm
Current Stability	100 nA	+0 … +7 nA
Timing	0 s	± 10s

Considering the worst cases we irradiated within a time range between 87 and 106 years. The greatest impact is the fluctuation in the proton current. Since it is under steady fluctuation around 100 nA depending on gas flow in the proton source and probe voltage, extraction voltage and lense voltage, it is very unlikely that the samples were irradiated with great discrepancies to 100 nA in average. The error range is set by the logged peak values.

4. RESULTS AND DISCUSSION

4.1. In-Situ Measurements

The experiment was split into two phases. In the first phase, we irradiated the samples with 100 keV protons with a current of 100 nA for approximately 26.6 min. In phase two, the proton irradiation was stopped. To estimate, if any detected effects only occur during proton irradiation, we observed the samples for another approximately 30 min under vacuum without radiation. Subsequently, the samples were removed from the sample chamber and placed in the airlock, which was flooded with nitrogen. This was to visibly confirm, if any major changes of the surface occur after venting the airlock in terms of oxidation when the sample is removed from the airlock. Due to geometric reasons, it was not possible to apply LAMBDA at the airlock. Therefore, Fig. 5 displays the recorded behavior of phase 1 and 2, but not for the venting of the airlock.

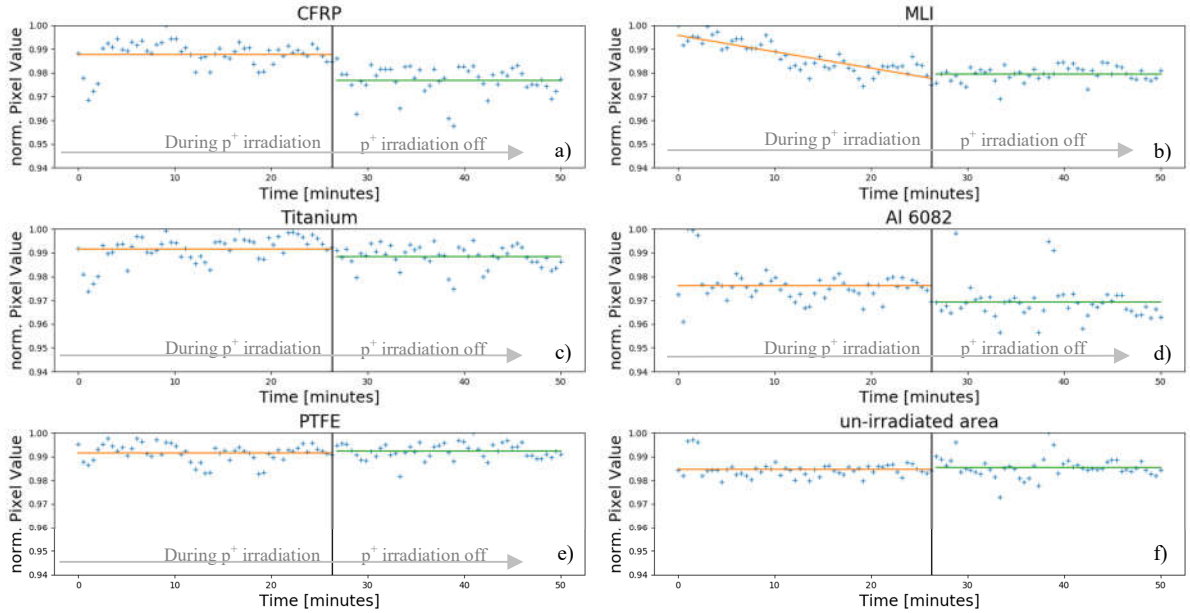

Fig. 5: Measurement results of LAMBDA

In general, the reflectivity/brightness changes are relatively small and do not change by more than 2.5%. Nonetheless, certain changes can be detected. In particular, the MLI sheet (panel b) of Fig. 5) showed a notable decrease in the reflected intensity during proton irradiation (phase 1). Furthermore, CFRP (panel a)) showed a constant brightness during proton irradiation but an intensity drop was observed when the radiation was turned off. This indicates that the material might have been glooming due to surfaces charging. The metallic samples (Titanium c), Al 6082 d)) as well as PTFE, panel e) showed no significant radiation-induced changes in their

reflectivity. AcktarBlack is a very absorptive material with an overall reflectivity < 2%. Therefore, its reflectivity could not be observed.

4.2. Microscopic Measurements

After releasing the target from the vacuum, it was immediately investigated with the digital microscope. We took measurements of the same samples and areas before and after the proton irradiation. At 200 times magnification, no structural damages due to protons were visible, see Fig. 6.

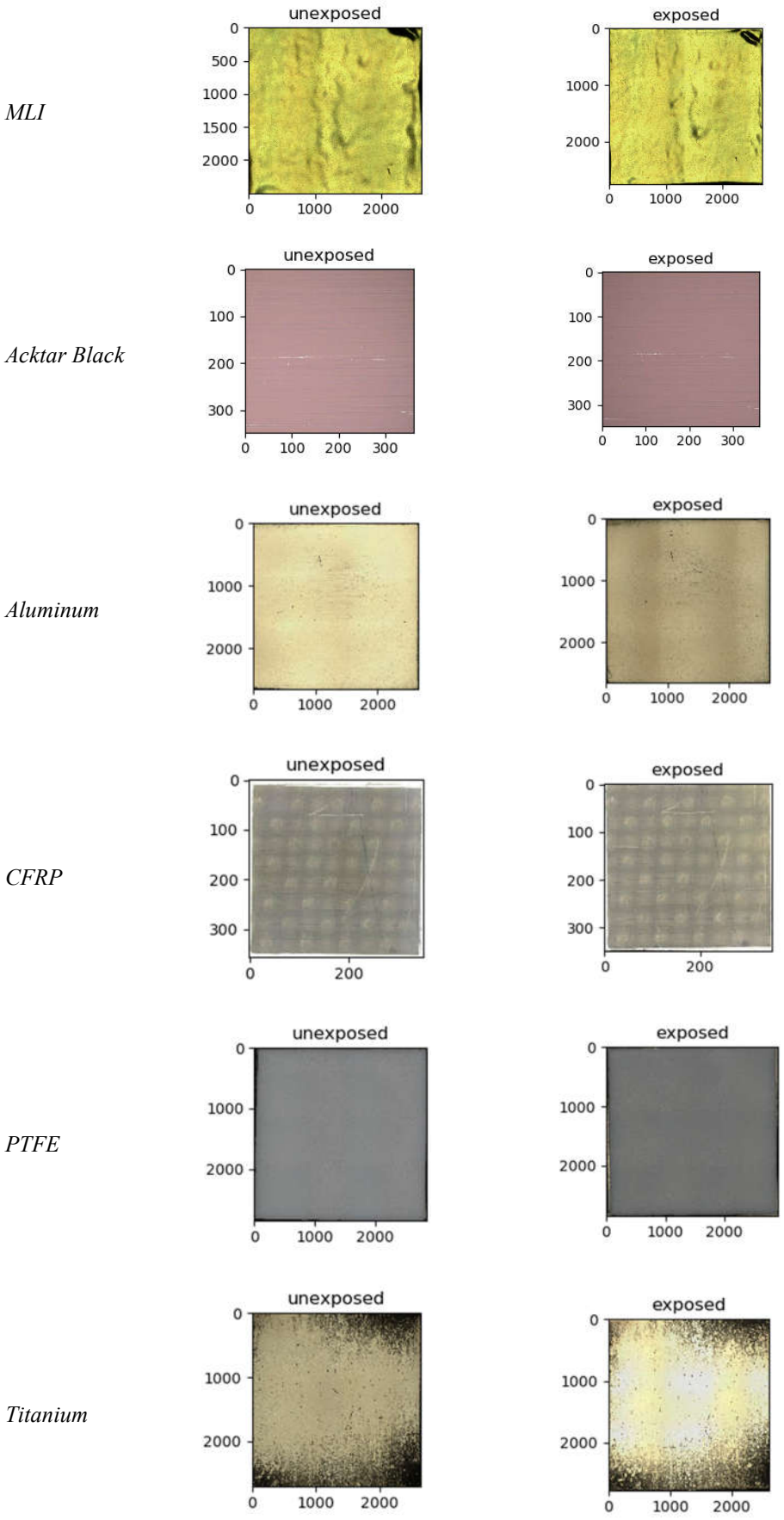

Fig. 6: Microscope images (sample size 21x21 mm²) of the samples before (left panel) and after (right panel) irradiation

Afterwards, the samples were investigated with a SEM. This allows for the investigation with a higher resolution. Here, we took a set of reference samples and compared them to the irradiated sample set. We found that samples containing organic polymers (CFRP and PTFE) showed radiation induced surface modifications, while metallic samples, including MLI, appeared unaffected by the proton irradiation. The detailed findings for PTFE and CFRP are as follows:

PTFE showed significant changes on the material surface structure, see Fig. 7. While the reference sample shows a plain structure with scratches and irregularities, the irradiated sample showed a very irregular surface which looks like melting patterns. As a thermoplastic with very low thermal conductivity and low radiative cooling ability due to its white appearance, melting seems to be a reasonable behavior.

Reference

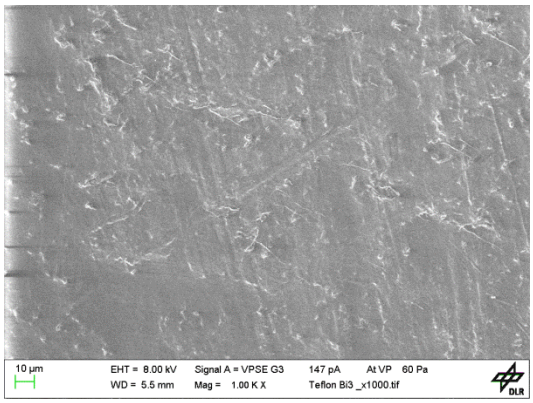

Irradiated Sample

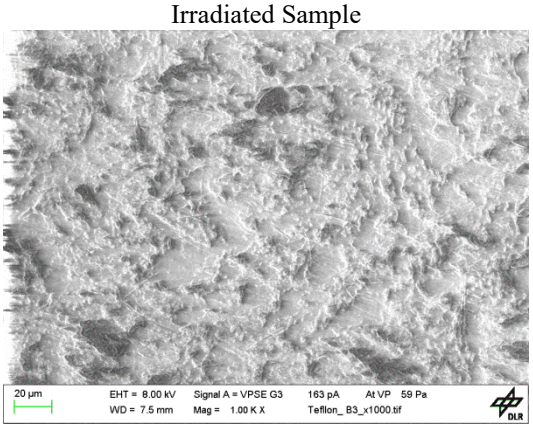

Fig. 7: Comparison of SEM image of the non-irradiated PTFE reference (left) and the proton irradiated sample (right)

CFRP was investigated for three conditions: changes in pure resin areas, changes in fiber dominated areas and changes in fiber-resin bonding, see Fig. 8. Major changes were found in the pure resin areas (panels a) and b)), where abrasion of the surface has occurred. The reference surface is mostly plain with sharp grains and a few mountains. For the irradiated sample, almost no sharp grains are detectable; the surface appears smoother. Regarding the fibers, panel c) and d) they appear with better contrast for the irradiated sample. This indicates abrasion of the resin since the fibers are usually covered with a thin layer of resin. Furthermore, the reference shows resin conglomerates on the fiber surface while the irradiated sample shows a plainer surface with breaking patterns along the fiber.
In the bonding area, panels e) and f), we can see fibers that are peaking out the resin for the irradiated sample. On the other side, for the references we see a blurry scheme of the fiber which indicates that it is still covered with a resin layer. We detected these results on several points on the sample surface.

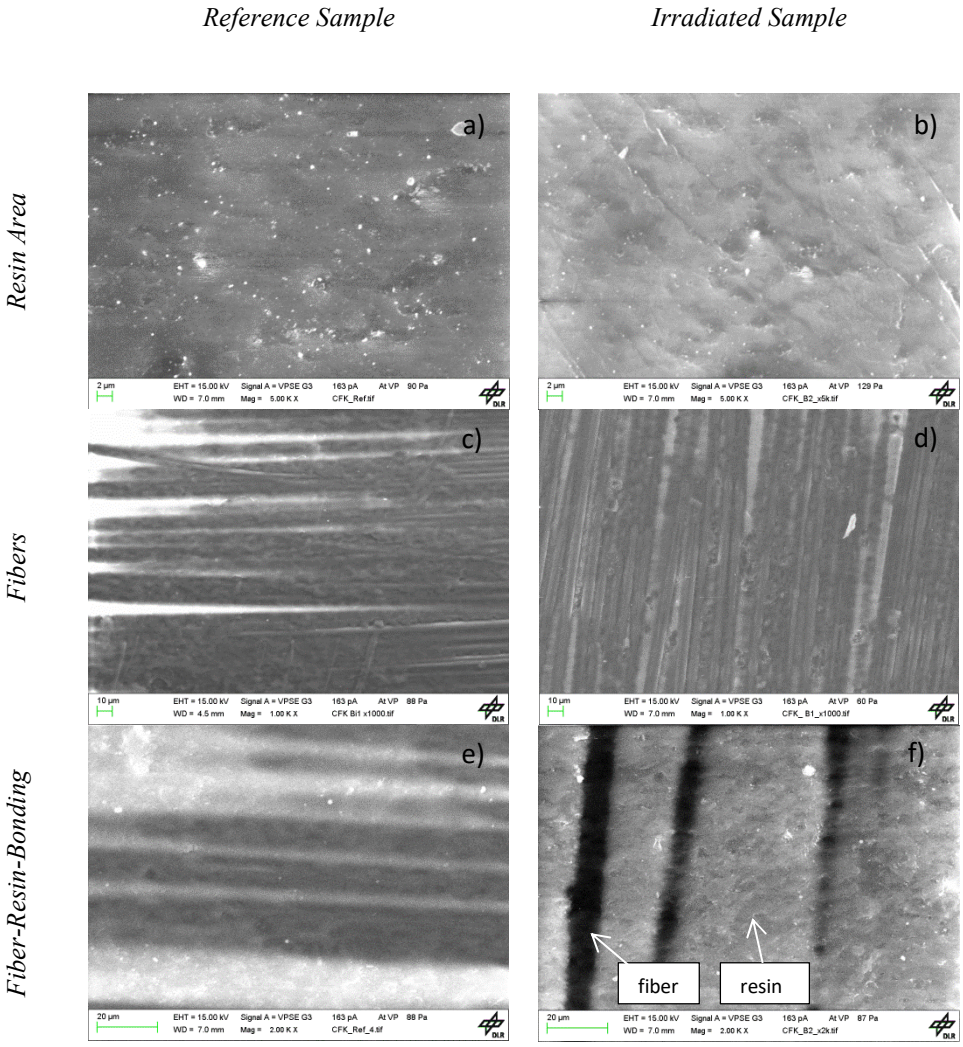

Fig. 8: SEM image of CFRP reference (left column) and sample (right column)

4.3. Spectral Analysis

We also investigated the wavelength dependent reflectance of samples at normal incidence with a Fourier Transform Infrared Spectrometer (FTIR), see Fig. 9. This allows for estimating possible wavelength depended color shifts due to proton related aging. Our reference is a copper mirror which is represented by the blue line. Its reflectivity is set to be 1 and all samples reflectivity is described relative to the copper mirror.

As it turned out, none of the samples undergo any measurable color shifts in the whole wavelength range. Nevertheless, we measured a significant change in relative reflectivity between the reference set and the irradiated sample set. Most significantly, we found a change in the reflectivity aluminum (red) and titanium (purple). The reflectivity of the irradiated samples stays below the reflectivity of the reference sample. The reflectivity of the irradiated samples is approximately 60% of the initial value of the reference sample. Since both sets have been treated by the same polishing procedure, this can either be explained by manufacturing discrepancies or by re-oxidation of the surfaces after irradiation. Re-oxidation processes for metals, especially for aluminum, are expectable. Also, since there is no visible modification on the sample surface that could cause a less reflective behavior, such as tiny scratches, we considered re-oxidation processes, which lead to a less reflective metal surface. This result would be consistent with the fact that we didn't measure reflectivity changes during proton irradiation.

Most interestingly is the behavior of MLI (rose). As we have measured before, its reflectivity has been reduced during the aging process. The purpose of MLI is to protect a satellite from rising temperatures due to thermal radiation, but we observe decay in reflectivity for the infrared range (wavenumbers smaller than 6000 cm^{-1}, panel b) and d)). It drops from 0.9 (panel b)) to less than 0.75 (panel d)).

On the other hand, polymer samples (orange, brown), including AcktarBlack (green), showed no variations in their spectral features. CFRP and AcktarBlack are black and therefore very absorptive, while PTFE is a white but very diffusive material, which is why they don't show any significant specular reflections. The infra-red

measurement shows a similar result like the visible with a peak for the CFRP, AcktarBlack and PTFE around 5800 cm^{-1}.

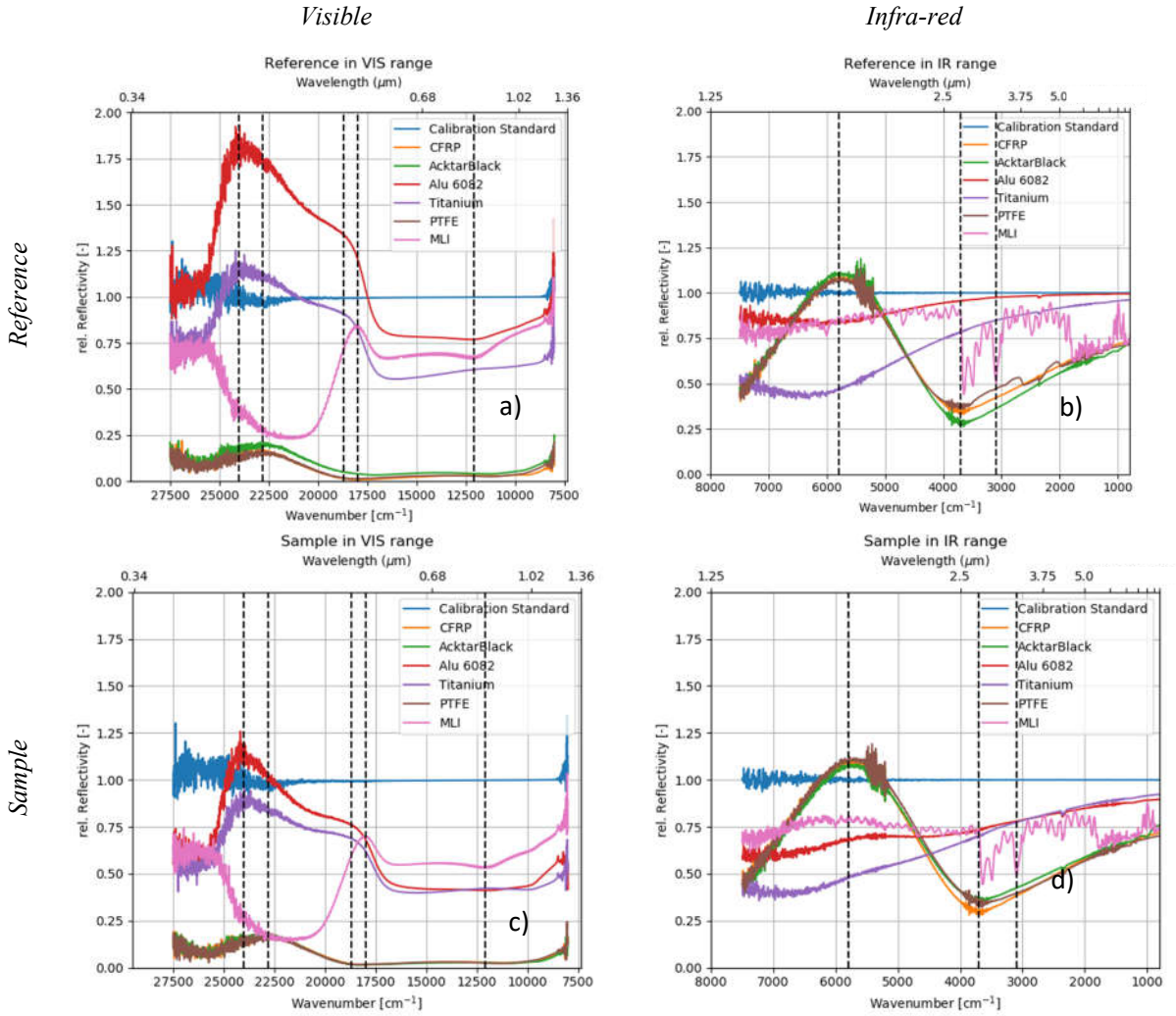

Fig. 9: Comparison of normal reflection response

5. CONCLUSIONS

We investigated the effects of low energetic proton irradiation equivalent to 800 km SSO LEO orbit on different types of material surfaces over a simulated time span of 100 years.
A microscopic analysis of the irradiated samples reveals that materials containing organic polymers Polytetrafluoroethylene (PTFE) and carbon fiber reinforced plastic (CFRP) show significant changes in surface morphology. These changes can be directly detected using scanning electron microscopy SEM. As opposed to this, no major changes in the surface morphology were detected for metallic surfaces such as aluminum, titanium, AcktarBlack or multi-layer insulation (MLI). Changes in optical properties where detected for MLI measured by LAMBDA and also affect the relative reflectivity as measured via FT-IR spectroscopy. To solidify our conclusion, we intend to extend our irradiation experiments towards lower proton energies (e.g. 10 keV) as well as to perform additional testing with low energetic electrons.

For further work, we intend to lower the proton energies based on space environmental beta-models to provoke more protons interacting with the surface as well as applying an equivalent energy by electrons.

6. ACKNOWLEDGEMENTS

The contributions from Dr. Patric Seefeldt, who supported our experiment during the corona lock-down, in the experimental procedure and in fruitful discussions of the gathered data are gratefully acknowledged. We also want to thank Samantha Siegert for proof reading the manuscript.

7. LITERATURE

[1] UNCOMPUOS, *Space Debris Mitigation Guidelines,* Inter-Agency Space Debris Coordination Committee, Inter-Agency Space Debris Coordination Committee, 2007.

[2] J.-C. Liou, P. D. Anz-Meador, J. N. Opiela and D. Shoots, "History of On-Orbit Satellite Fragmentations, 15th Edition," 2018.

[3] L. Newman, M. Hejduk, R. Frigm and M. Duncan, "Evolution and Implementation of the NASA Robotic Conjunction Assessment Risk Analysis Concept of Operations," in *Advanced Maui Optical and Space Surveillance Technologies Conference*, 2014.

[4] A. Rossi and G. B. Valsecchi, "Collision risk against space debris in Earth orbits," *Celestial Mechanics and Dynamical Astronomy,* vol. 95, pp. 345-356, 5 2006.

[5] J. C. Liou, A. K. Anilkumar, B. Bastida, T. Hanada, H. Krag, H. Lewis, M. Raj, M. Rao, A. Rossi and R. Sharma, "Stability of the future LEO environment–an IADC comparison study," in *Proceedings of the 6th European Conference on Space Debris*, 2013.

[6] J.-C. Liou, A. K. Anilkumar, B. Virgili, T. Hanada, H. Krag, H. Lewis, M. Raj, M. Rao, A. Rossi and R. Sharma, "STABILITY OF THE FUTURE LEO ENVIRONMENT – AN IADC COMPARISON STUDY," 2013.

[7] D. Hand, D. Tyler, S. Murali, M. Roggemann and N. Peterson, "Real Time Polarization Light Curves for Space Debris and Satellites," 9 2010.

[8] G. C. Giakos, R. H. Picard, P. D. Dao and P. Crabtree, "Object detection and characterization by monostatic ladar Bidirectional Reflectance Distribution Function (BRDF) using polarimetric discriminants," in *Electro-Optical Remote Sensing, Photonic Technologies, and Applications III*, 2009.

[9] H. Kurosaki, T. Yanagisawa and A. Nakajima, "Observation of Light Curves of Space Objects," in *Advanced Maui Optical and Space Surveillance Technologies Conference*, 2009.

[10] D. Hall, K. Hamada, T. Kelecy and P. Kervin, "Satellite Surface Characterization from Non-resolved Multi-band Optical Observations," in *Advanced Maui Optical and Space Surveillance Technologies Conference*, 2012.

[11] M. C. Polo, I. Vaughn, A. Alenin, A. Lambert, D. Griffin, R. Boyce and S. Tyo, "On-Sky Evaluation of Passive Polarimetry as a Technique to Characterise Space Debris," in *7th European Conference on Space Debris*, 2017.

[12] V. E. Skurat, E. A. Barbashev, Y. I. Dorofeev, A. P. Nikiforov, M. M. Gorelova and A. I. Pertsyn, "Simulation of polymer film and surface behaviour in a space environment," *Applied Surface Science,* vol. 92, pp. 441-446, 1996.

[13] Dennison, J. L. Prebola, A. Evans, D. Fullmer, J. L. Hodges, D. H. Crider and D. S. Crews, "Comparison of Flight and Ground Tests of Environmental Degradation of MISSE-6 SUSpECS

Materials," in *11th Spacecraft Charging Technology Conference*, 2010.

[14] D. P. Engelhart, R. Cooper, H. Cowardin, J. Maxwell, E. Plis, D. Ferguson, D. Barton, S. Schiefer and R.Hoffmann, "Space Weathering Experiments on Spacecraft Materials," in *2017 Advanced Maui Optical and Space Surveillance Technologies Conference (AMOS)*, 2017.

[15] M. Sznajder, U. Geppert and M. Dudek, "Degradation of metallic surfaces under space conditions, with particular emphasis on Hydrogen recombination processes," *Advances in Space Research,* vol. 27, 4 2015.

[16] C. M. Nöldeke, The Space Radiation Environment, epubli, 2017.

[17] S. Scharring, J. Rodmann and W. Riede, "Network performance analysis of laser-optical tracking for space situational awareness in the Lower Earth Orbit," in *2019 Advanced Maui Optical and Space Surveillance Technologies Conference (AMOS)*, 2019.

[18] T. Renger, M. Sznajder and U. Geppert, "Experimental Studies of low energy Proton Irradiation of thin vacuum deposited Aluminum Layers," 2014.

[19] T. Renger, M. Sznajder, A. Witzke and U. Geppert, "The Complex Irradiation Facility at DLR-Bremen," *Journal of Materials Science and Engineering A,* vol. 4, 7 2014.

[20] M. Sznajder, U. Geppert and M. R. Dudek, "Hydrogen blistering under extreme radiation conditions," *npj Materials Degradation,* vol. 2, pp. 1-8, 2018.

[21] M. Sznajder, P. Seefeldt, T. Spröwitz, T. Renger, J. H. Kang, R. Bryant and W. Wilkie, "Solar sail propulsion limitations due to hydrogen blistering," *Advances in Space Research,* 2020.

[22] D. Heynderickx, B. Quaghebeur and H. D. R. Evans, "The ESA Space Environment Information System (SPENVIS)," in *IAF abstracts, 34th COSPAR Scientific Assembly*, 2002.

[23] D. Mehrholz, L. Leushacke, W. Flury, R. Jehn, H. Klinkrad and M. Landgraf, "Detecting, tracking and imaging space debris," *ESA Bulletin(0376-4265),* p. 128–134, 2002.

[24] J. Eastment, D. Ladd, P. Donnelly, A. Ash, N. Harwood, I. Ritchie, C. Smith, J. Bennett, M. Rutten and N. Gordon, "Technical Description of Radar and Optical Sensors Contributing to Joint UK-Australian Satellite Tracking, Data-fusion and Cueing Experiment," in *Advanced Maui Optical and Space Surveillance Technologies Conference*, 2014.